Supplemental Material

SUPPLEMENTAL METHODS

Derivation of patient and disease-specific hiPSCs. Patient-specific hiPSCs were generated from dermal fibroblasts as previously reported using lentivirus on Matrigel-coated tissue culture dishes (BD Biosciences, San Jose, CA) with mTESR-1 hESC Growth Medium (STEMCELL Technologies, Vancouver, Canada) [1].

HEK293 cell culture. HEK293 cells stably expressing hERG were grown in Minimum Essential Medium (MEM) supplemented with 10% heat inactivated FBS, non-essential amino acids (1×), Sodium Pyruvate (1×), Penicillin-Streptomycin (100 U/ml and 100 U/ml), and G418 (500 μg/ml) (Gibco). In preparation for electrophysiological recordings, cells were trypsinized, washed in standard MEM media, and plated onto coverslips 1-2 days before recordings.

Dissociation of beating EBs into single hESC-CMs and hiPSC-CMs for electrophysiological recordings. Dissociation of beating EBs was conducted as previously described [2]. Briefly, spontaneously contracting EBs were mechanically collected, enzymatically dispersed into single cells and attached to Matrigel-coated glass coverslips (CS-22/40, Warner, Hamden, CT). 5-10 days after plating, stably contracting single hESC-CMs/hiPSC-CMs were subjected to patch clumping as described below.

Quantitative real-time PCR. Total mRNAs were isolated from hESC-CMs, control iPSC-CMs, disease-specific hiPSC-CMs, HEK293 cells stably expressing hERG (hERG-HEK293),

blank HEK293, and human left ventricular tissue (LV) using the Qiagen RNeasy Mini kit. 1 μg of RNA was used to synthesize cDNA using the *Superscript II* First-Strand cDNA synthesis kit (Invitrogen). 0.25 μL of the reaction was used to quantify gene expression by qPCR using *TaqMan* Universal PCR *Master Mix*. Expression values were normalized to the average expression of housekeeping gene GAPDH.

Teratoma formation. $1x10^6$ undifferentiated hiPSCs were suspended in 10 ul Matrigel (BD Biosciences) and delivered by a 28.5 gauge syringe to the renal capsule of 8 week old SCID Beige mice. Eight weeks after cell delivery, tumors were explanted for hematoxylin and eosin (H&E) staining.

Immunofluorescence staining. Immunofluorescence was performed using appropriate primary antibodies and AlexaFluor conjugated secondary antibodies (Invitrogen) as previously described [3]. The primary antibodies used in this study were Tra-1-60, Tra-1-81, SSEA-4, Oct 4, Nanog (Santa Cruz, CA), Sox2 (Biolegend, San Diego, CA), sarcomeric α-actinin (Sigma, St. Louis, MO), cTnT (Thermo Scientific Barrington, IL), Myosin light chain 2a (MLC2a), and Myosin light chain 2v (MLC2v) (Synaptic Systems, Goettingen, Germany).

Electrophysiological recordings of HEK293 cells. Traditional whole-cell voltage-clamp recording was performed at room temperature to record the hERG currents in HEK293 cells with an EPC-10 amplifier (HEKA, Germany). The pipette solution contained 130 mM KCl, 1 mM $MgCl_2$, 10 mM HEPES, 5 mM Mg-ATP, 5 mM EGTA (pH 7.25 with KOH at 25°C); the

external solution contains 137 mM NaCl, 4 mM KCl, 1 mM $MgCl_2$, 10 mM glucose, 1.8 mM $CaCl_2$, and 10 mM HEPES (pH 7.4 with NaOH at 25°C). Capacitance and 60–80% series resistance were routinely compensated. The cells were voltage clamped at a holding potential of -80 mV. The hERG current was activated by depolarizing at +20 mV for 2 sec, after which the current was taken back to -50 mV for 2 sec to remove the inactivation and observe deactivation of the tail current. The first step at -50 mV was used as a baseline for measuring the tail current peak amplitude. After achieving whole-cell configuration, the cells were monitored for 90 sec to assess stability and washed with external solution for 60 sec. The voltage protocol described above was then applied to the cells every 20 sec throughout the whole procedure. Only stable cells with recording parameters above threshold were allowed to enter the drug treatment phase. External solution containing 0.1% DMSO (vehicle) was applied to cells to establish the baseline. After allowing the current to stabilize for 3 min, single cells were treated with drug compound solution as defined in the Methods section of the manuscript. Recordings of hERG current were maintained until the compound's effect reached a steady state or for a maximum of 6 min. Washout with external solution was performed until the recovery of the current reached a steady state.

Electrophysiological recordings of hESC-CMs and hiPSC-CMs. To record spontaneous action potential recordings from hESC-CMs and hiPSC-CMs, a Giga-Ohm seal was achieved under the voltage-clamp mode and the APs were collected under the current-clamp configuration using an EPC-10 amplifier (HEKA, Germany). Contracting embryoid bodies (EBs) were mechanically isolated, enzymatically dispersed into single cells and attached to

0.1% gelatin-coated glass coverslips (Warner Instruments, CS-8R, USA). While recordings, the coverslips containing plated cardiomyocytes were transferred to a RC-26C recording chamber (Warner, USA) mounted on to the stage of an inverted microscope (Nikon, Tis, Japan). The glass pipettes were prepared using thin-wall borosilicate glass (A-M System, Catalog # 617000, USA) using a micropipette puller (Sutter Instrument, P-97, USA), polished using a microforge (Narishige, MF830, Japan) and had resistances between 2-4 MΩ. Extracellular solution perfusion was continuous using a rapid solution exchanger (Biologic, RC-200, USA) with solution exchange requiring ~1 min. Temperature was maintained constantly by a TC-324B heating system (Warner, USA) at 36 - 37 °C. Data were acquired using PatchMaster software (HEKA, Germany), digitized at 1.0 kHz and were analyzed using PulseFit (HEKA, Germany), Igor Pro (Wave Metrics), Microcal Origin 6.1 (OringinLab), or Prism 5 (GraghPad). The recordings were conducted in normal Tyrode solution containing 140 mM NaCl, 5.4 mM KCl, 1 mM MgCl2, 10 mM glucose, 1.8 mM $CaCl_2$, and 10 mM HEPES (pH 7.4 with NaOH at 25°C). The pipette solution contained 120 mM KCl, 1 mM $MgCl_2$, 10 mM HEPES, 3 mM Mg-ATP, and 10 mM EGTA (pH 7.2 with KOH at 25°C). For recordings on differentiated ventricular-like cardiomycytes, the maximum diastolic potential (MDP) of single cardiomyocytes varied from −70 mV to −50 mV, action potential amplitude (APA) was greater than 90 mV, and action potential duration $(APD)_{90}/APD_{50}$ was less than 1.20. Only those cardiomyocytes satisfying the above criteria were considered to be ventricular-like cardiomyocytes and selected for drug screening. Escalating doses were sequentially applied to isolated single hESC-CMs and hiPSC-CMs. Steady-state was obtained for 3 min before application of higher doses. The average responses of 20 APs were analyzed

for each dose. The steady-state before and after application were used to calculate the percentage of APD_{90} prolongation/shortening at each dose. Dose-response data were fit to Hill equation. IC_{50} here is defined the half maximal inhibitory concentration to block the hERG peak tail current or significantly prolong the APD_{90}. Significant APD_{90} prolongation is defined as a >10% change in APD_{90} at the indicated concentration [4].

SUPPLEMENTAL FIGURE LEGENDS

Supplemental Figure 1. Sequence analysis of patient-specific LQT, HCM, and DCM hiPSCs for KCNQ1, MYH7, and TNNT mutant loci. **(a)** Schematic pedigrees of the LQT, HCM and DCM families used in this study. Squares represent male family members and circles represent female family members. Solid and open symbols indicate presence and absence of the familial LQT, HCM, and DCM mutations, respectively. For the LQT cohort, hiPSCs were derived from three patients carrying the G269S mutation in KCNQ1 (II-1, II-2, and III-1) and one family-matched healthy individual (II-3). For the HCM cohort, hiPSCs were derived from three patients carrying the R663H mutation in MYH7 (I-1, II-1, and II-3) and one family matched control (II-2). For the DCM cohort, hiPSCs were derived from three patients carrying the R173W mutation in TNNT2 (I-1, I-2, and II-1) and one family-matched control (II-2). **(b)** Confirmation of the G269S missense mutation on exon 6 of the KCNQ1 gene in LQT patients (3 patient lines) by PCR and sequence analysis. **(c)** Confirmation of the R663H missense mutation on exon 18 of the MYH7 gene in HCM patients (3 patient lines) by PCR and sequence analysis. **(d)** Confirmation of the R173W missense mutation on exon 12 of the TNNT gene in DCM patients (3 patient lines) by PCR and sequence analysis.

Supplemental Figure 2. Transgene silencing in patient-specific hiPSCs. Quantitative PCR ratios for total versus endogenous expression of the reprogramming factors OCT4, SOX2, MYC and KLF4 in hESCs, control hiPSCs, LQT hiPSCs, HCM hiPSCs, and DCM hiPSCs.

Supplemental Figure 3. Pluripotency of patient-specific hiPSCs as demonstrated by teratoma formation. Representative H&E staining of a solid teratoma transplanted under the

renal capsule of an immunodeficient mouse show presence of cellular derivatives belonging to 3 germ layers including brain (ectoderm), skeletal muscle (mesoderm), and gut epithelium (endoderm).

Supplemental Figure 4. Cardiac differentiation efficiencies of patient-specific hiPSC lines. (a) Cardiac differentiation efficiency of control, LQT, HCM, and DCM hiPSC-CMs was measured by the % of beating EBs (n=50 per line, 3 lines per cohort)**. (b)** Quantification of TNNT2-positive cardiomyocytes derived from control, LQT, HCM, and DCM hiPSC lines (n=50 per line, 3 lines per cohort).

Supplemental Figure 5. Capacitance measurements for patient-specific hiPSC-CM lines. Quantification of capacitance values for single hESC-CMs, control hiPSC-CMs, LQT hiPSC-CMs, HCM hiPSC-CMs, and DCM hiPSC-CMs by patch clamp recordings (n=45-60, 3 lines per cohort). ** indicates $P<0.01$, as compared to control hiPSC-CMs.

Supplemental Figure 6. Electrophysiological profiling of disease-specific hiPSC-CMs. (a) Quantification of nodal-like, atrial-like, and ventricular-like APD_{90}/APD_{50} in hESC-CMs, control hiPSC-CMs, LQT hiPSC-CMs, HCM hiPSC-CMs, and DCM hiPSC-CMs. **(b)** Quantification of nodal-like, atrial-like, and ventricular-like V_{max} in hESC-CMs, control hiPSC-CMs, LQT hiPSC-CMs, HCM hiPSC-CMs, and DCM hiPSC-CMs. Please note the smaller V_{max} values for nodal-like cardiomyocytes. **(c)** Quantification of nodal-like, atrial-like, and ventricular-like MDP in hESC-CMs, control hiPSC-CMs, LQT hiPSC-CMs, HCM

hiPSC-CMs, and DCM hiPSC-CMs. **(d)** Quantification of nodal-like, atrial-like, and ventricular-like overshoot in hESC-CMs, control hiPSC-CMs, LQT hiPSC-CMs, HCM hiPSC-CMs, and DCM hiPSC-CMs.

Supplemental Figure 7. Inter-comparison of electrophysiological baselines for family-matched control hiPSC-CMs belonging to LQT, HCM, and DCM cohorts. (a-c) APD_{50}, APD_{70}, and APD_{90} for each of the three myocyte subtypes (nodal-, atrial- and ventricular-like) in control hiPSC-CMs derived from healthy individuals belonging to LQT, HCM and DCM family cohorts. **(d)** Percentage of DADs and EADs observed in control hiPSC-CM lines derived from healthy individuals belonging to LQT, HCM and DCM family cohorts.

Supplemental Figure 8. Stability of HEK293 hERG tail currents. Peak tail currents were measured for a representative HEK-293 cell expressing hERG. Treatment with 0.1% DMSO (vehicle control) had no effect on hERG tail currents over an observation period of 8,000 seconds (n=3). The arrowhead indicates the time point at which 0.1% DMSO added.

Supplemental Figure 9. Comparison of APD_{90}-dose relationship between hESC-CMs and control hiPSC-CMs for verapamil and alfuzosin. (a) Upper panel: dose-response relationship of the steady-state APD_{90} prolongation for hESC-CMs and control hiPSC-CMs following treatment with verapamil. Data were fit by the Hill function. Lower panel: IC_{50} values of APD_{90} prolongation for hESC-CMs and control hiPSC-CMs following treatment with verapamil (n=9, 3 lines). **(b)** Upper panel: dose-response relationship of the steady-state

APD_{90} for hESC-CMs and control hiPSC-CMs following treatment with alfuzosin. Data were fit by the Hill function. Lower panel: IC_{50} values of APD_{90} prolongation for hESC-CMs and control hiPSC-CMs following treatment with alfuzosin (n=9, 3 lines).

Supplemental Figure 10. Electrophysiological stability of hiPSC-CM APs during vehicle treatment. Control hiPSC-CMs were treated with 0.1% DMSO (vehicle control) for 10 minutes. Representative traces are shown at time 0, 1 minute, 2 minutes, 5 minutes, 8 minutes, and 10 minutes (black, red, blue, purple, magenta and cyan, respectively) (n=6, 3 lines).

Supplemental Figure 11. Concentration-dependent block of hERG by cisapride in hERG expressing HEK293 cells. (a) Representative time course for treatment of a hERG expressing HEK293 cell at the following concentrations of cisapride: 1 nM, 10 nM, 30 nM, 100 nM, 300 nM, and 1 μM. **(b)** Representative traces showing the effect of cisapride on blockade of hERG current at doses of 0 nM, 1 nM, 10 nM, 30 nM, 100 nM, 300 nM, and 1 μM (black, red, blue, purple, magenta, cyan and green traces, respectively). Dose-dependent inhibition of hERG current was clearly observed. **(c)** Dose-response relationship showing steady-state inhibition of hERG by cisapride. IC_{50} was calculated by fitting a Hill function to the data constrained to 100% inhibition. IC_{50} for cisapride was 0.032 ± 0.003 μM (n=5 for each dose).

Supplemental Figure 12. Inter-comparison of cisapride and nicorandil-induced cardiotoxicity for family-matched control hiPSC-CMs belonging to LQT, HCM, and DCM cohorts. (a) Dose-response relationship showing steady-state prolongation of APD_{90} by cisapride for family-matched control hiPSC-CM lines derived from healthy subjects belonging to LQT, HCM and DCM cohorts. **(b)** IC_{50} values of APD_{90} prolongation of cisapride for control hiPSC-CM lines derived from LQT, HCM and DCM family cohorts. **(c)** Dose-response relationship showing steady-state shortening of APD_{90} by nicorandil for control hiPSC-CMs derived from LQT, HCM and DCM family cohorts. **(d)** IC_{50} values of nicorandil-induced APD_{90} shortening for control hiPSC-CM lines derived from LQT, HCM, and DCM family cohorts.

Supplemental Figure 13. Schematic for personalized approach to determination of drug-induced cardiotoxicity. Patient-specific somatic cells are reprogrammed to pluripotency by defined factors, differentiated to cardiac lineages and screened for drug response. Dosages and patient-specific toxicities can be calibrated based upon *in vitro* readouts of cardiotoxicity such as APD prolongation or induction of EADs/DADs at the single cell level.

Supplemental Video 1. Representative video of beating EBs generated by cardiac differentiation in suspension.

Supplemental Video 2. Representative video of the contracting cardiomyocytes dissociated from beating EBs.

SUPPLEMENTAL REFERENCES

1. Sun N, Yazawa M, Liu J, Han L, Sanchez-Freire V, Abilez OJ, Navarrete EG, Hu S, Wang L, Lee A, Pavlovic A, Lin S, Chen R, Hajjar RJ, Snyder MP, Dolmetsch RE, Butte MJ, Ashley EA, Longaker MT, Robbins RC, Wu JC. Patient-specific induced pluripotent stem cells as a model for familial dilated cardiomyopathy. *Science Translational Medicine*. 2012;4:130ra147

2. Yang L, Soonpaa MH, Adler ED, Roepke TK, Kattman SJ, Kennedy M, Henckaerts E, Bonham K, Abbott GW, Linden RM, Field LJ, Keller GM. Human cardiovascular progenitor cells develop from a kdr+ embryonic-stem-cell-derived population. *Nature*. 2008;453:524-528

3. Jia F, Wilson KD, Sun N, Gupta DM, Huang M, Li Z, Panetta NJ, Chen ZY, Robbins RC, Kay MA, Longaker MT, Wu JC. A nonviral minicircle vector for deriving human ips cells. *Nat Methods*. 2010;7:197-199

4. Redfern WS, Carlsson L, Davis AS, Lynch WG, MacKenzie I, Palethorpe S, Siegl PK, Strang I, Sullivan AT, Wallis R, Camm AJ, Hammond TG. Relationships between preclinical cardiac electrophysiology, clinical qt interval prolongation and torsade de pointes for a broad range of drugs: Evidence for a provisional safety margin in drug development. *Cardiovascular Research*. 2003;58:32-45

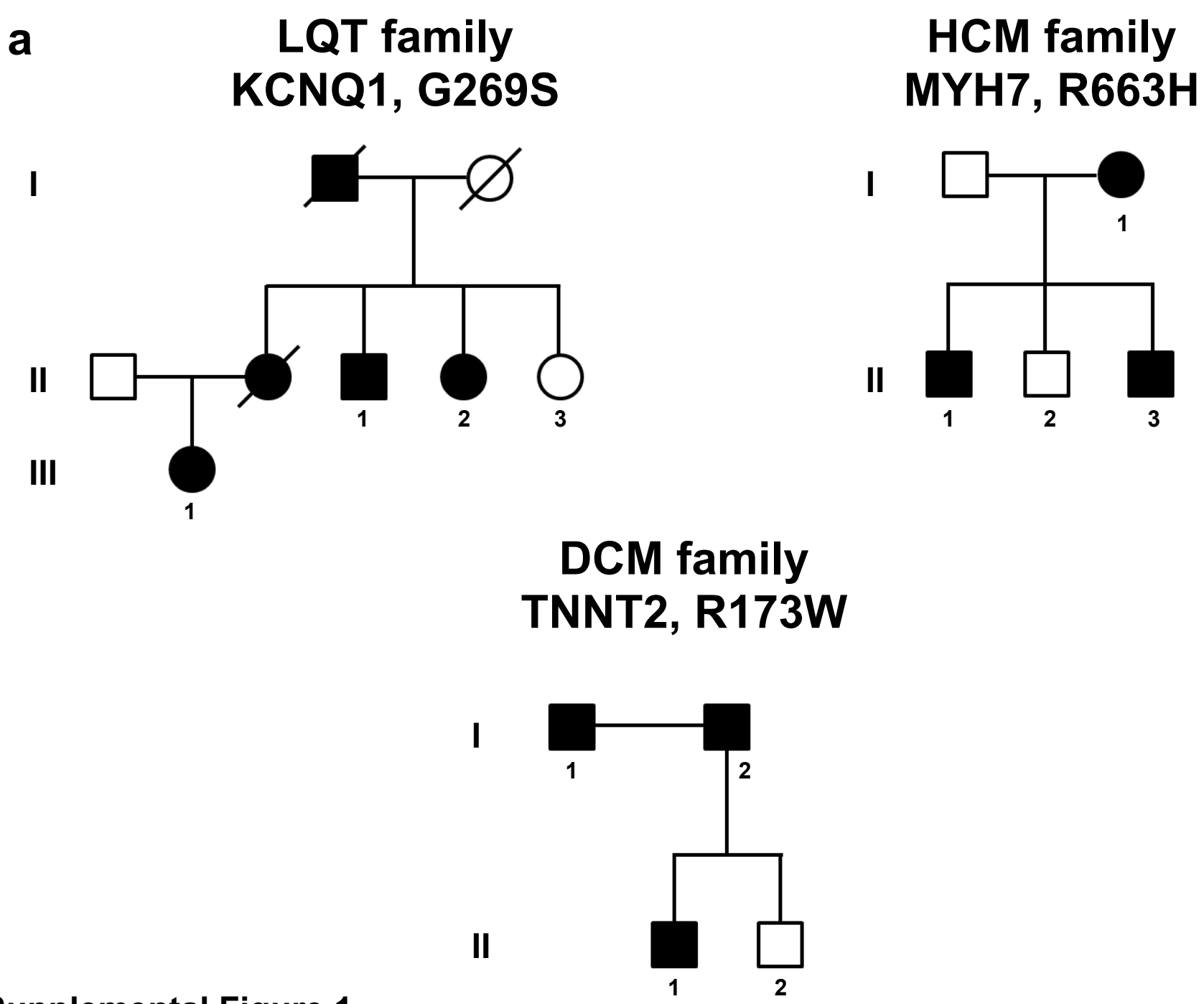

Supplemental Figure 1

b

LQT KCNQ1 G269S G-A

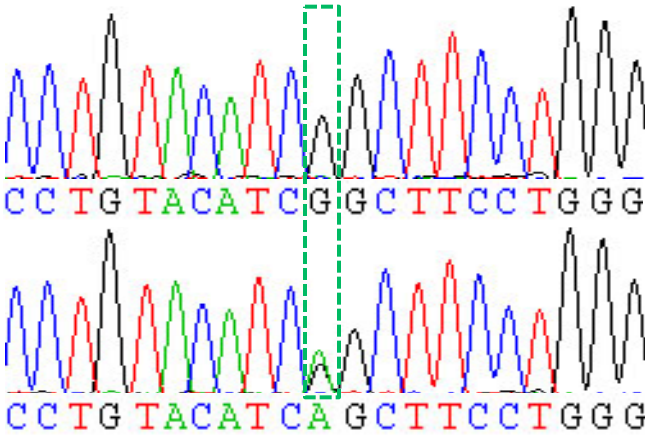

c

HCM MYH7 R663H G-A

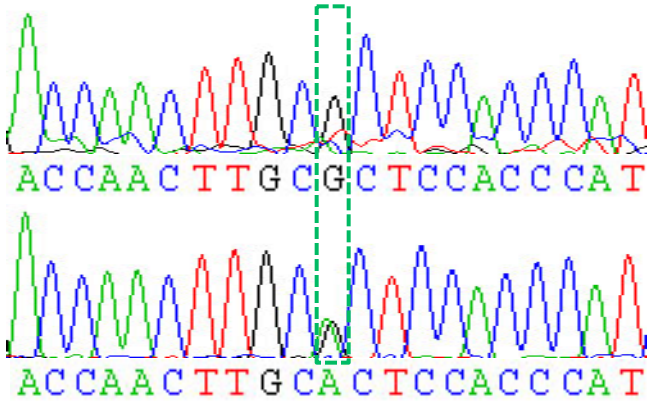

d

DCM TNNT2 R173W C-T

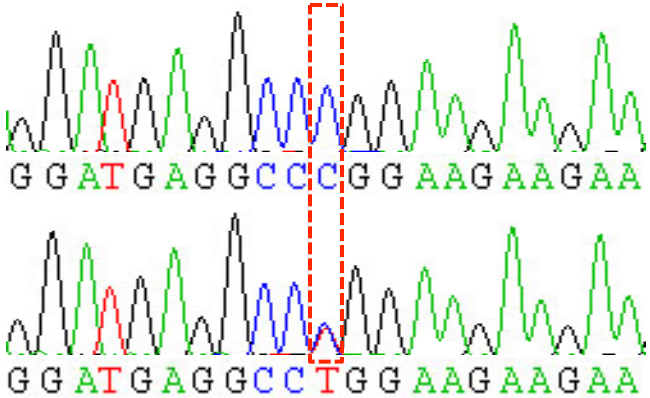

Supplemental Figure 1

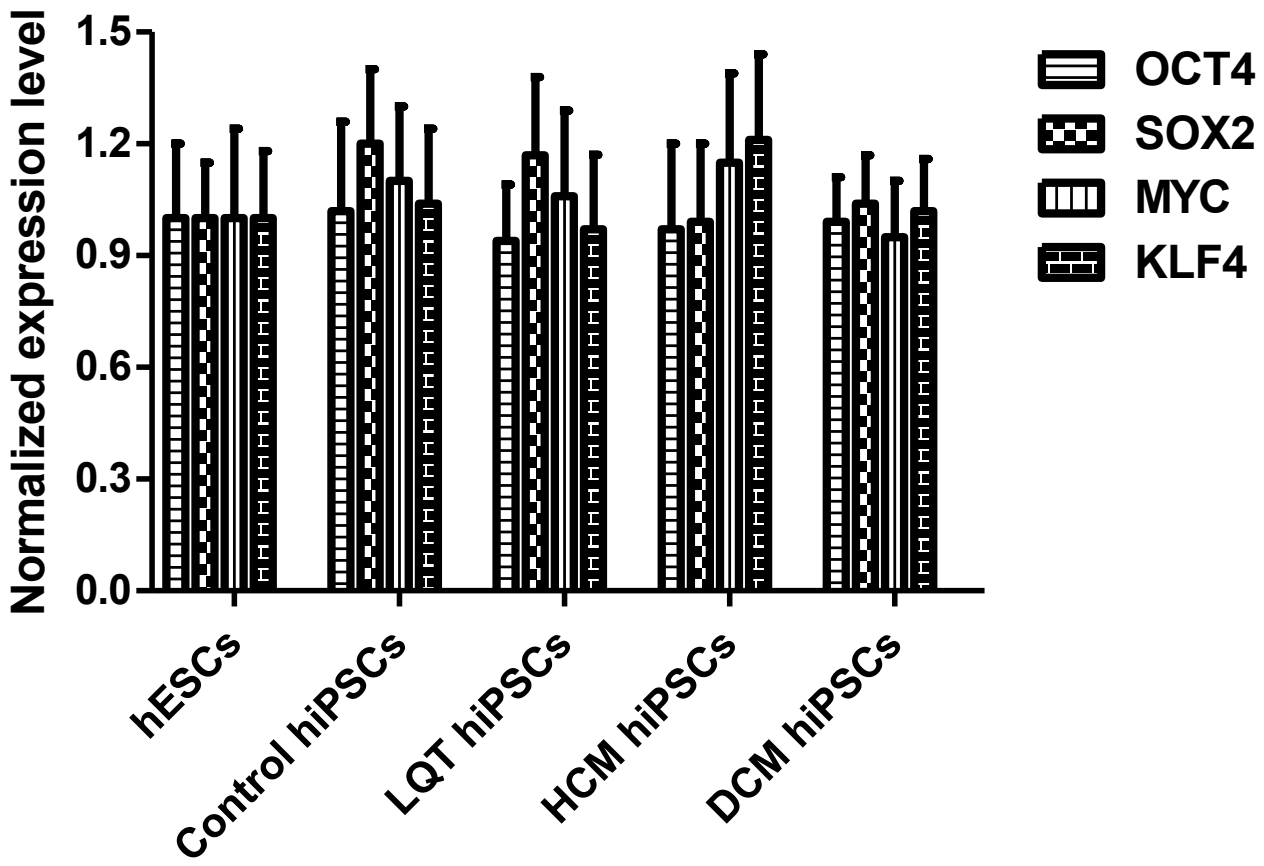

Supplemental Figure 2

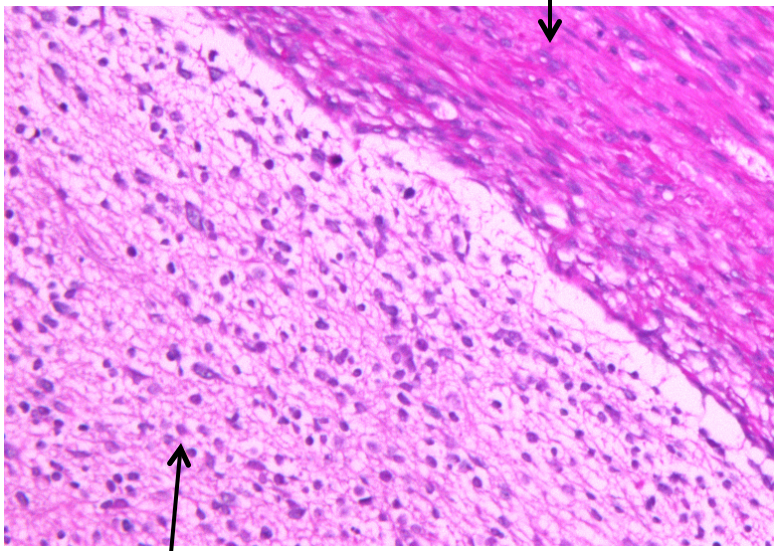

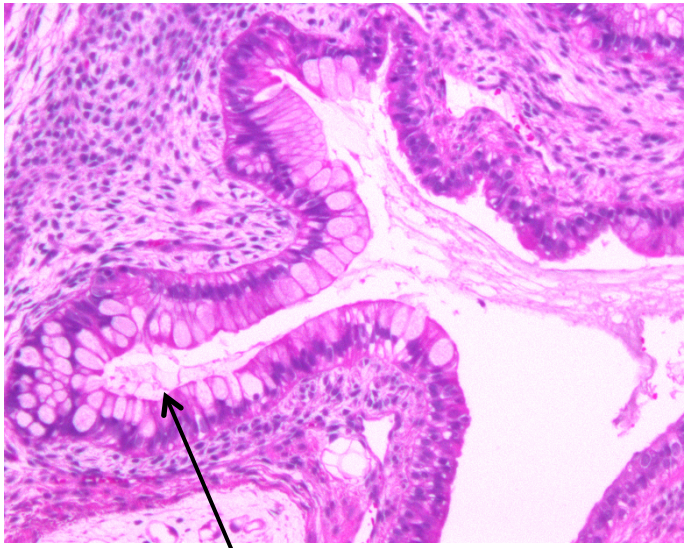

Supplemental Figure 3

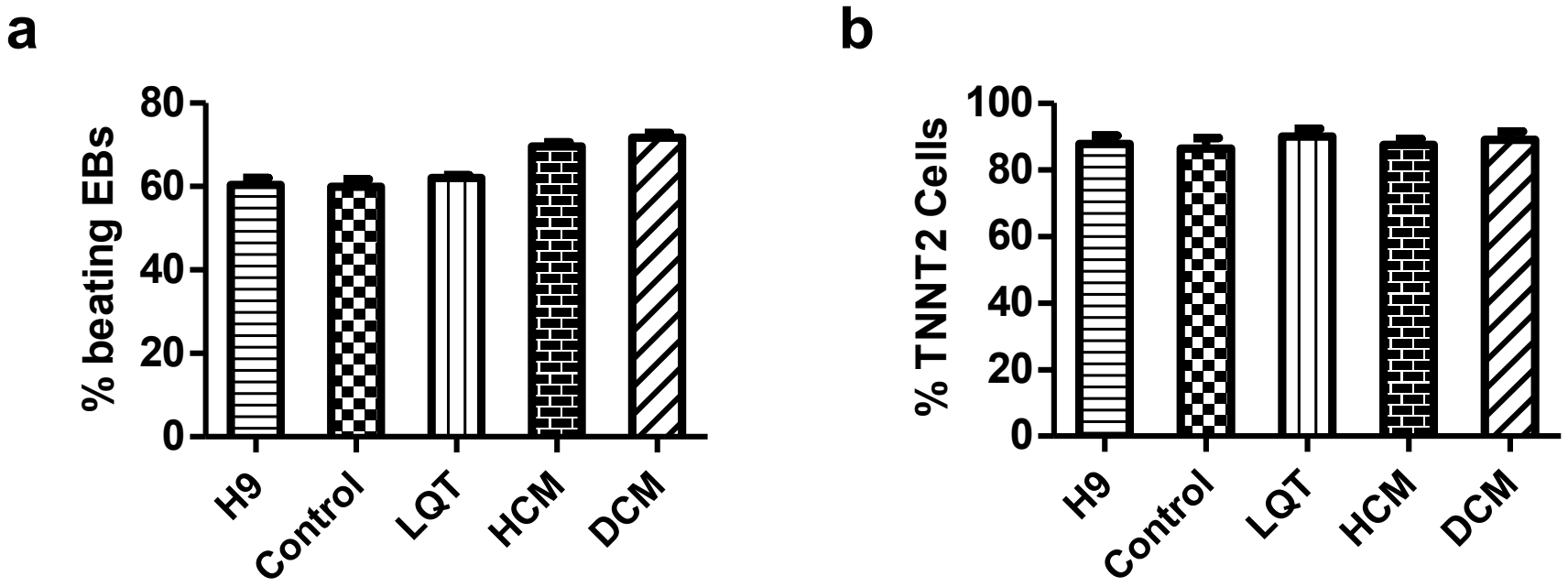

Supplemental Figure 4

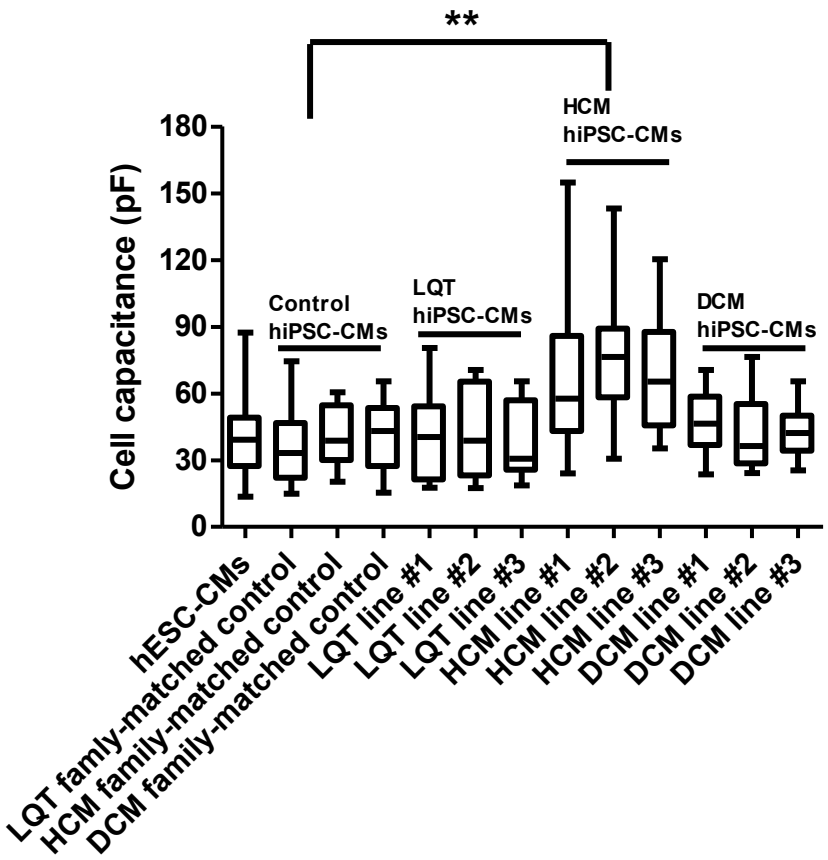

Supplemental Figure 5

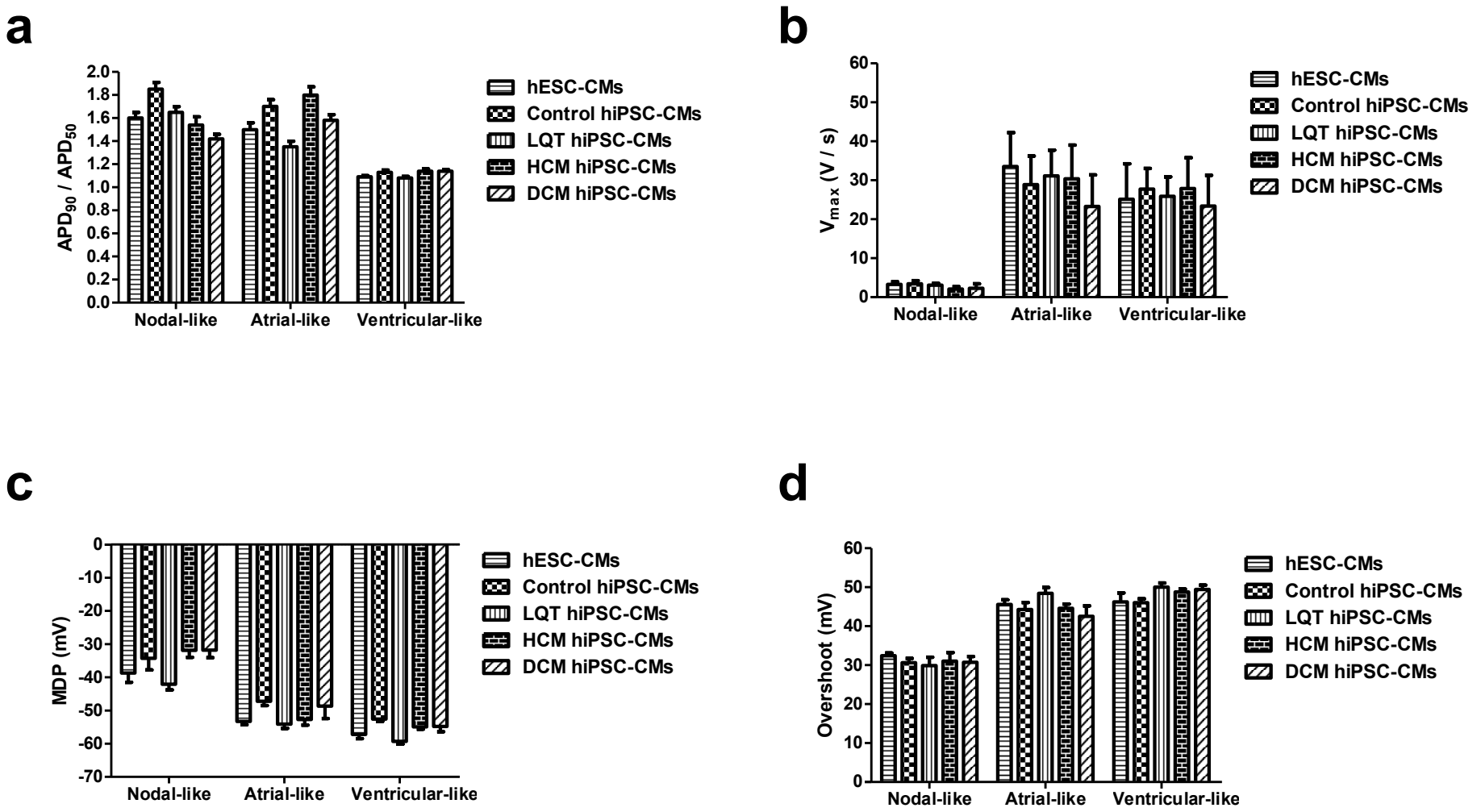

Supplemental Figure 6

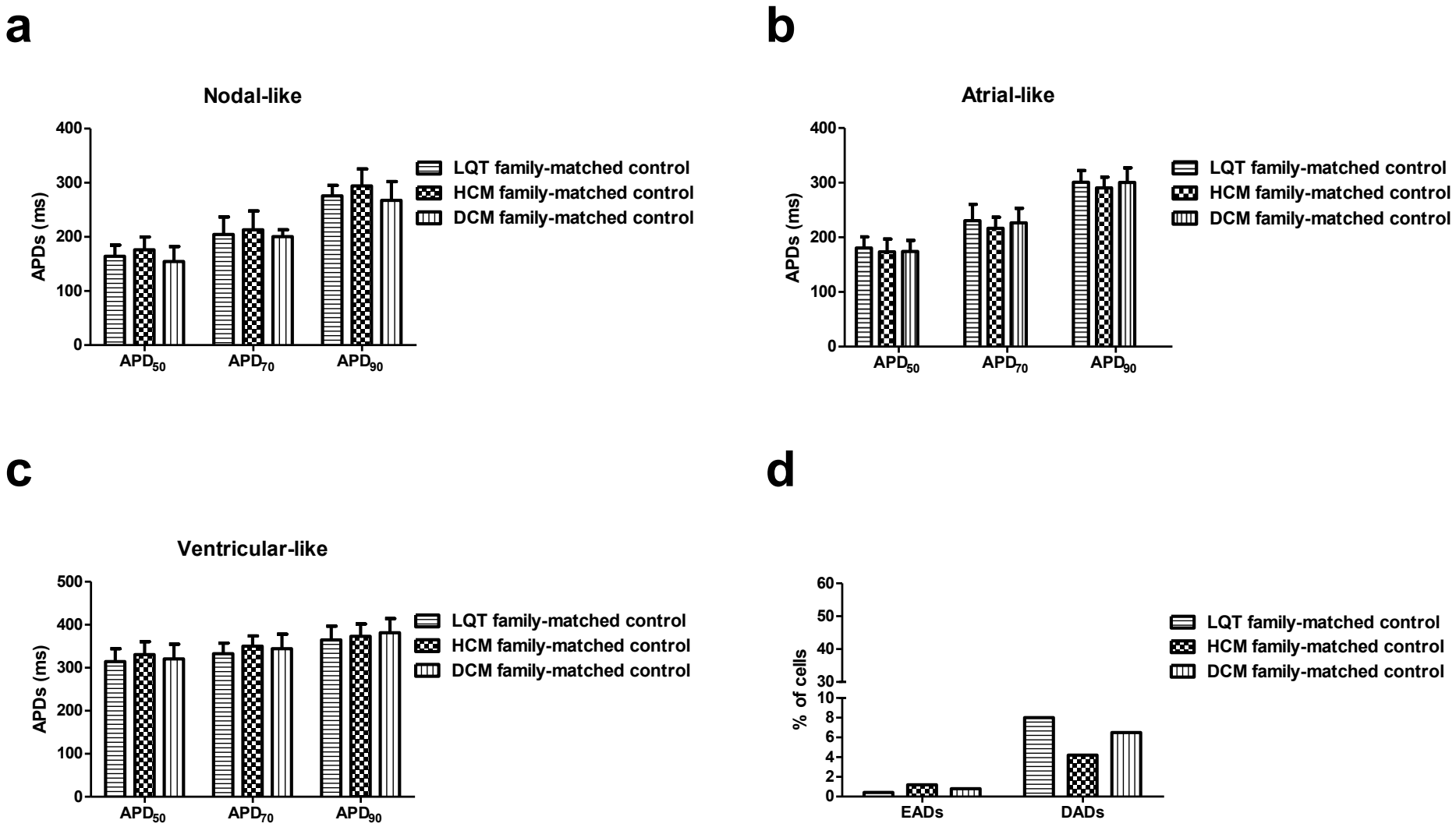

Supplemental Figure 7

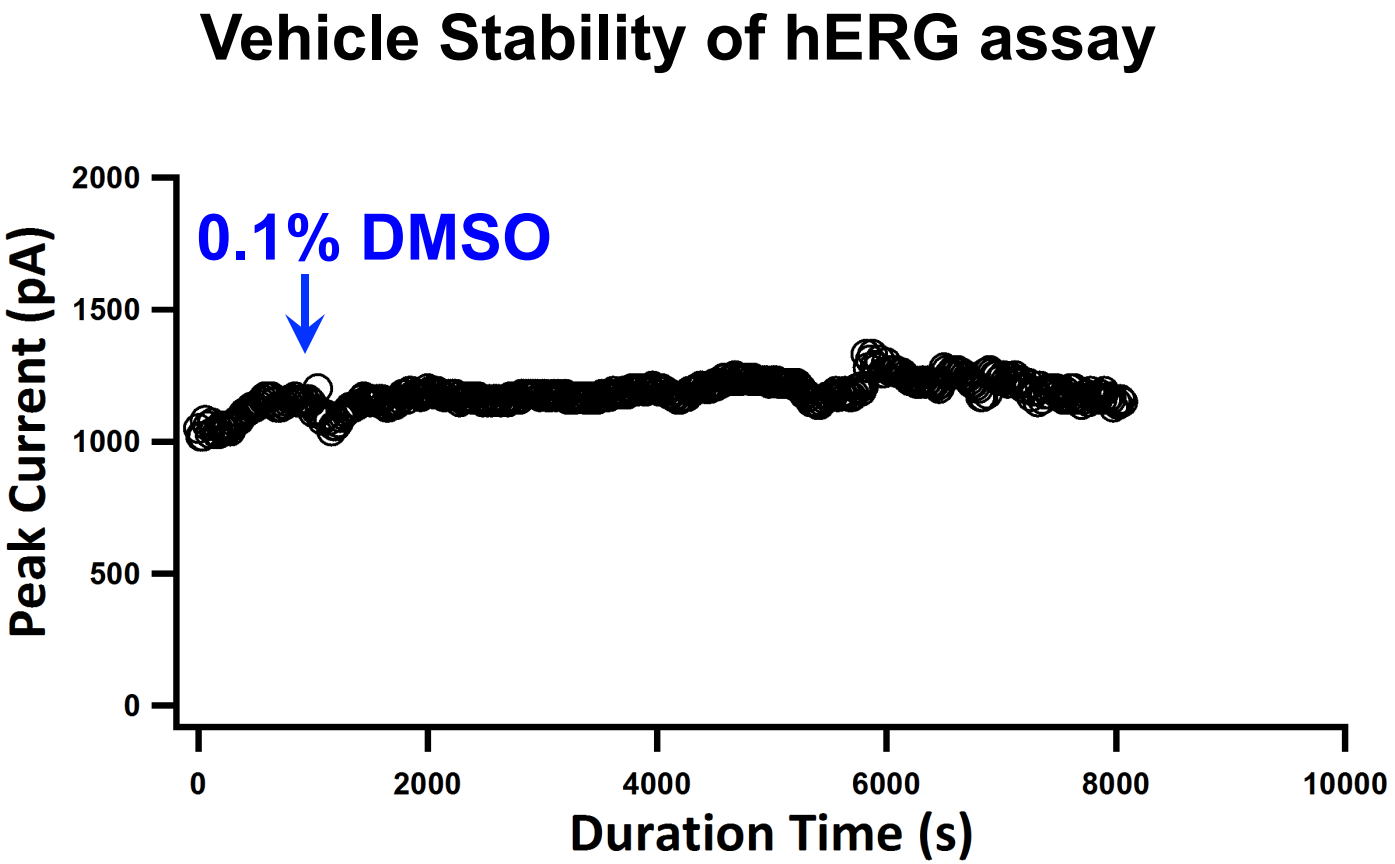

Supplemental Figure 8

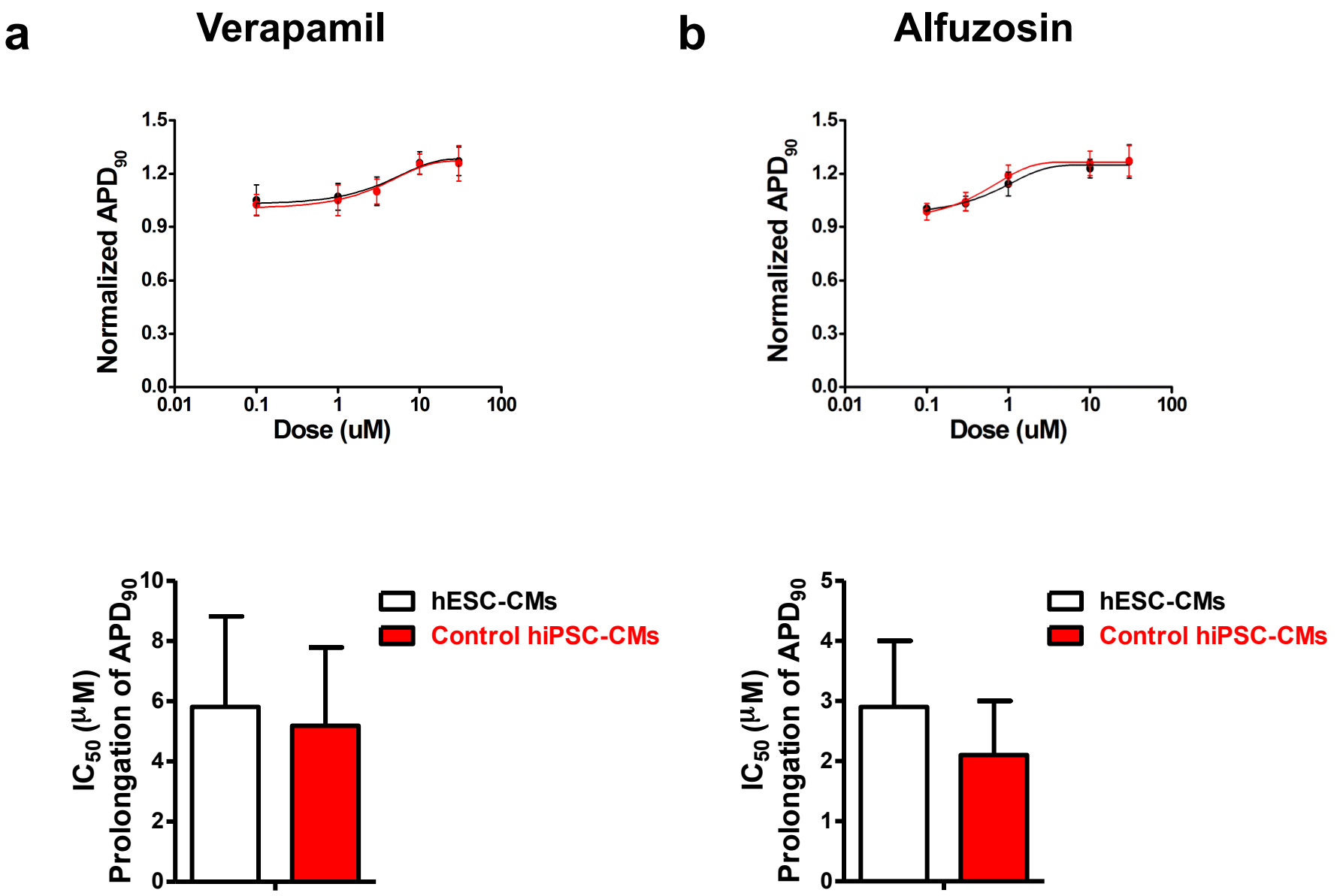

Supplemental Figure 9

Vehicle Stability of AP/hiPSC-CM assay

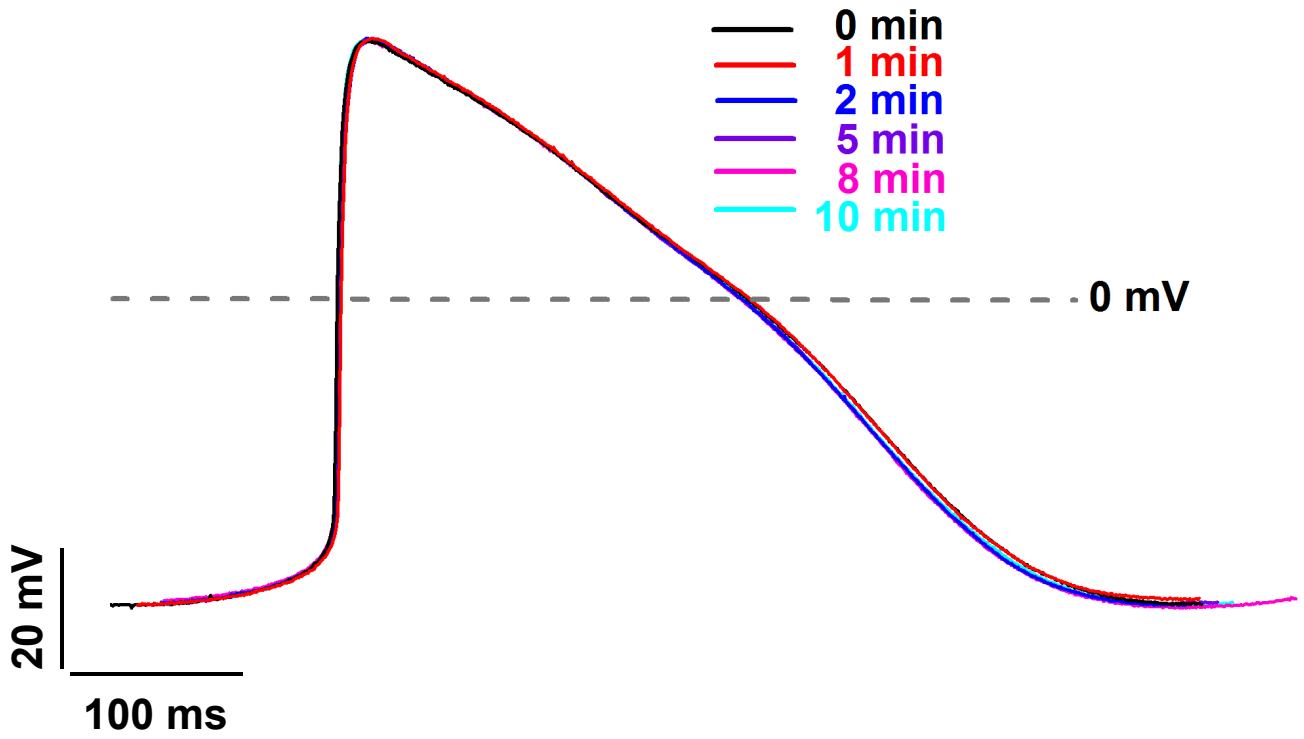

Supplemental Figure 10

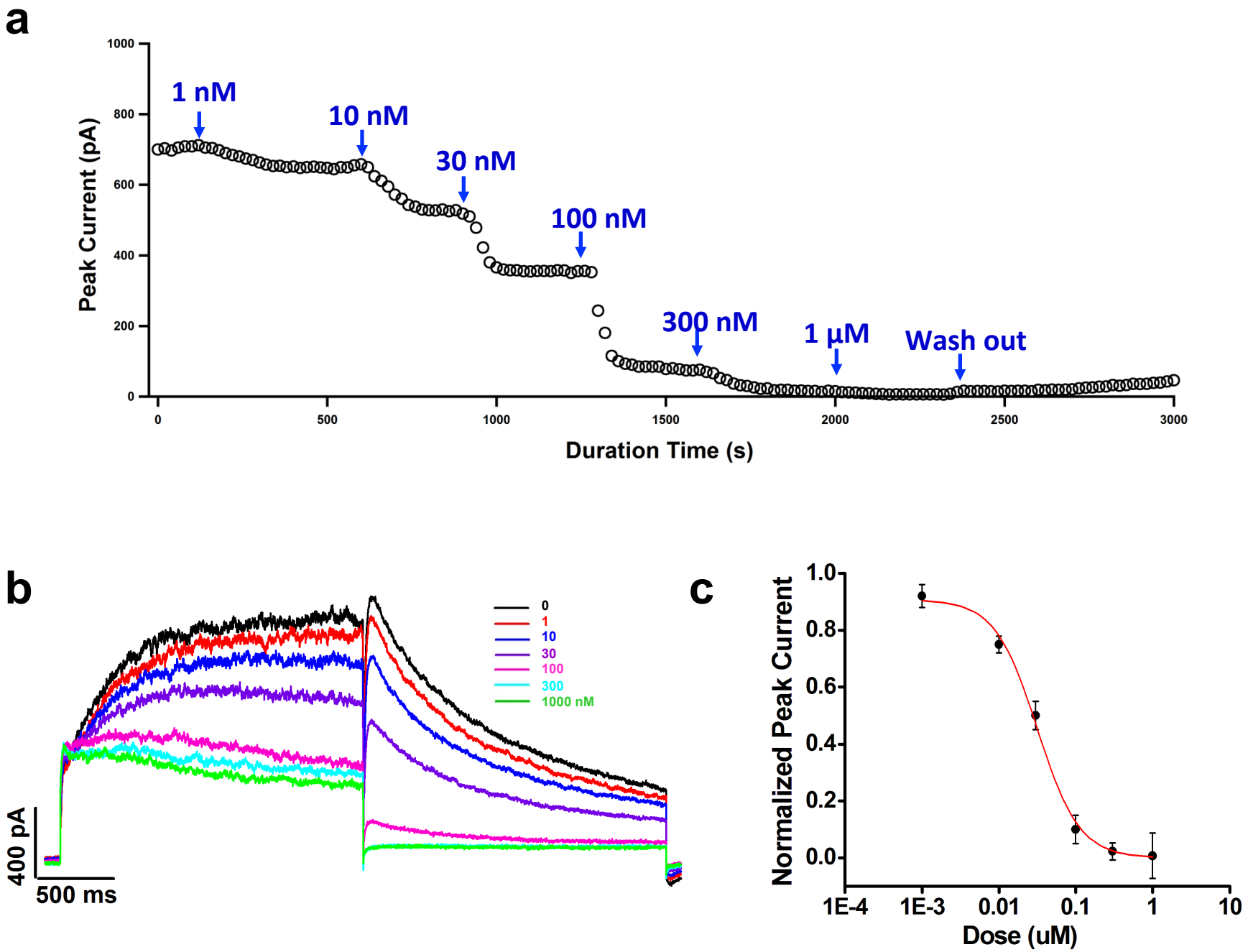

Supplemental Figure 11

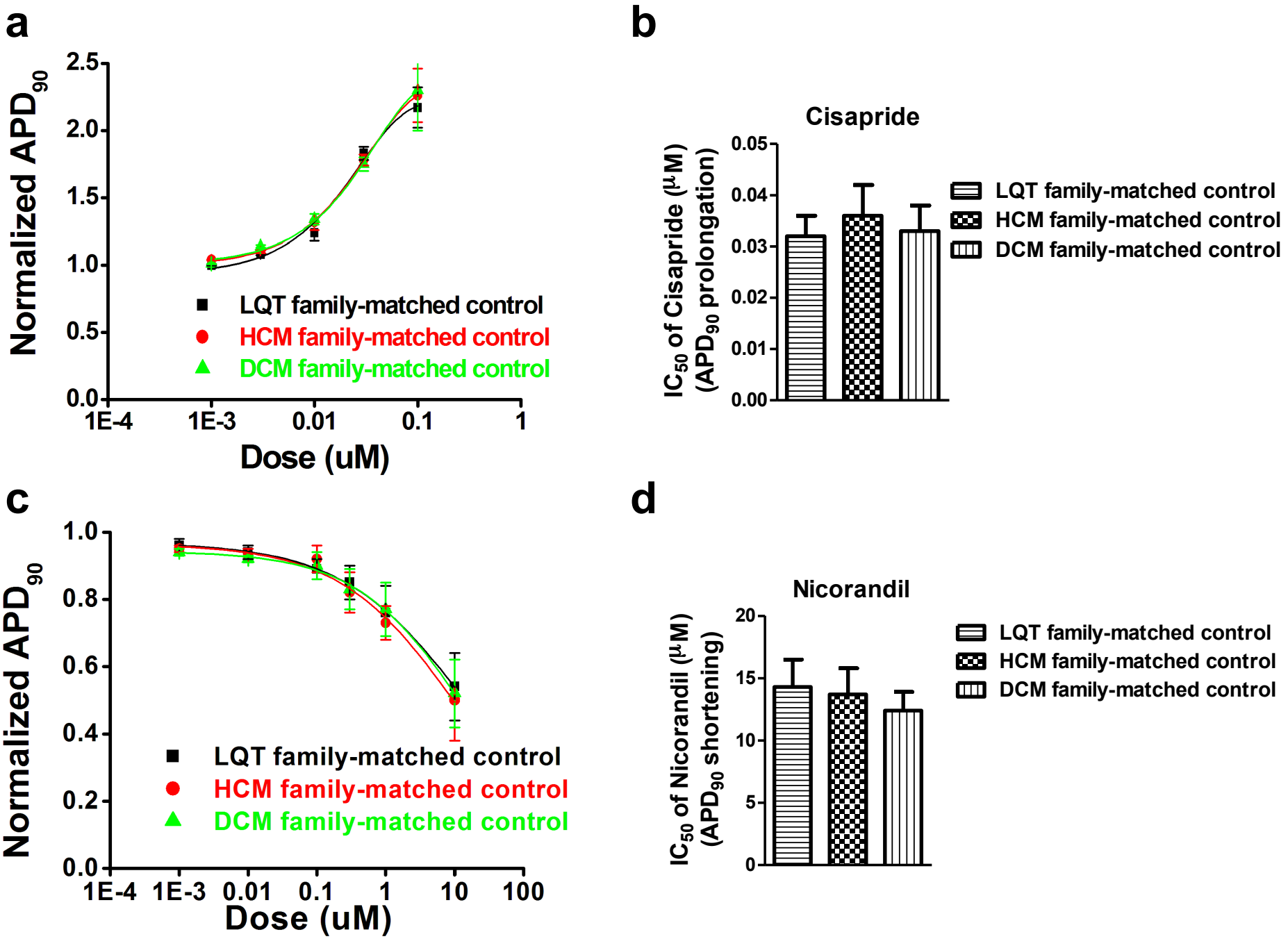

Supplemental Figure 12

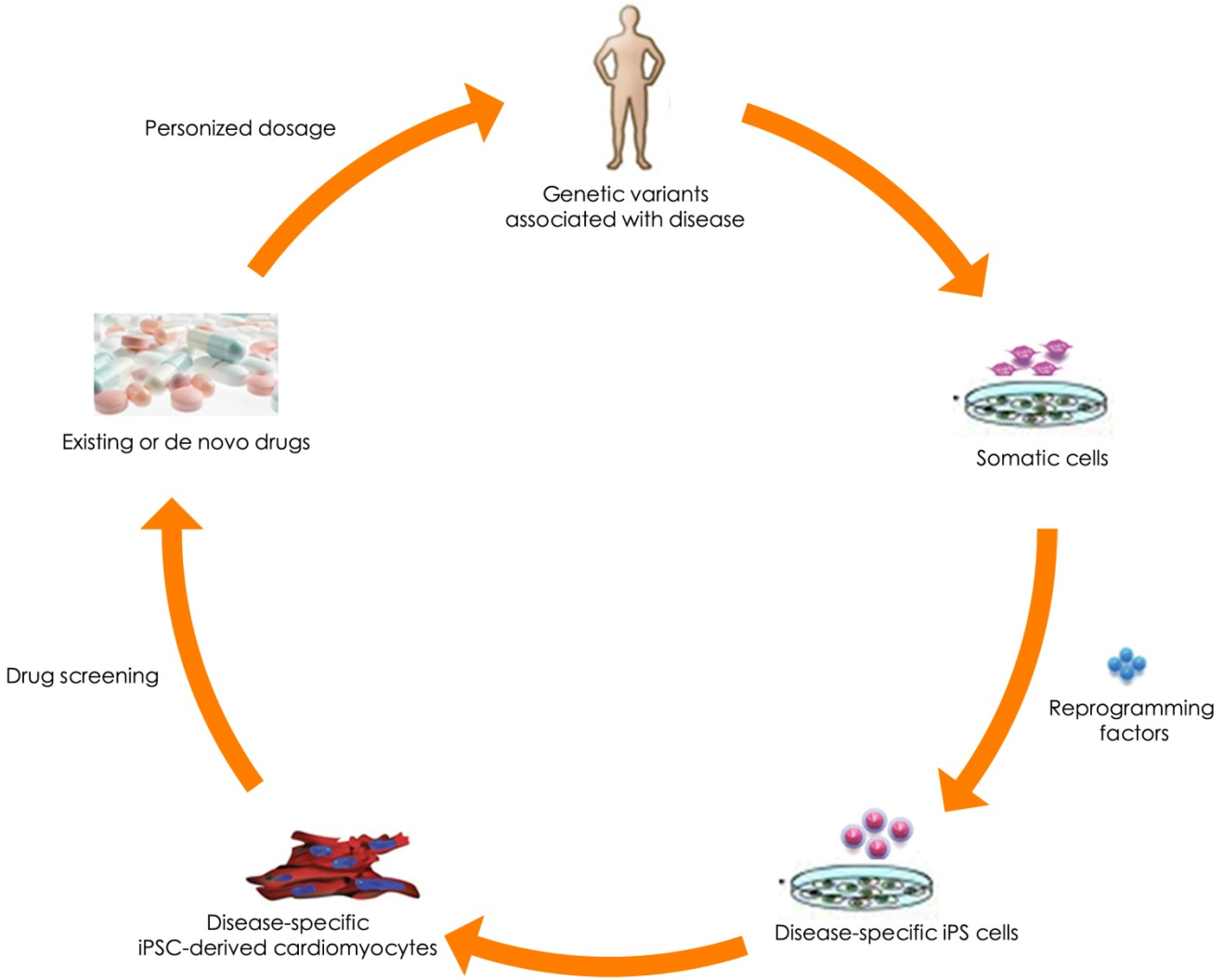

Supplemental Figure 13

Supplemental Table 1. Panel of hiPSCs from cardiovascular disease-specific patients and healthy controls for drug screening

	Genetic cause	Number of clones/patient-specific lines
Human ESCs (H9)	None	1
Control hiPSCs	None	3
LQT hiPSCs	KCNQ1 G269S	3
HCM hiPSCs	MYH7 R663H	3
DCM hiPSCs	TNNT2 R173W	3

Supplemental Table 2. Panel of LQT, HCM and DCM genes for genetic screening

Gene Symbol	Protein Coded	NCBI Ref Gene No.	Cell line/Mutation(s)				
			H9	Control	LQT	HCM	DCM
ACTC1	alpha-cardiac actin	NG_007553	None	None	None	None	None
CAV3	caveolin 3	NG_008797	None	None	None	None	None
GLA	galactosidase alpha	NG_007119	None	None	None	None	None
LAMP2	lysosomal-associated membrane protein 2	NG_007995	None	None	None	None	None
MTTG	mitochondrial transfer RNA glycine	NC_012920_TRNG	None	None	None	None	None
MTTI	mitochondrial transfer RNA isoleucine	NC_012920_TRNI	None	None	None	None	None
MTTK	mitochondrial transfer RNA lysine	NC_012920_TRNK	None	None	None	None	None
MTTQ	mitochondrial transfer RNA glutamine	NC_012920_TRNQ	None	None	None	None	None
MYBPC3	cardiac myosin-binding protein C	NG_007667	None	None	None	None	None
MYH7	beta-myosin heavy chain	NG_007884	None	None	None	R663H	None
MYL2	myosin regulatory light chain 2	NG_007554	None	None	None	None	None
MYL3	myosin light chain 3	NG_007555	None	None	None	None	None
PRKAG2	5'-AMP-activated protein kinase subunit gamma-2	NG_007486	None	None	None	None	None
TNNC1	troponin C	NG_008963	None	None	None	None	None
TNNI3	cardiac muscle troponin I	NG_007866	None	None	None	None	None
TNNT2	cardiac muscle troponin T	NG_007556	None	None	None	None	R173W
TPM1	alpha tropomyosin	NG_007553	None	None	None	None	None
TTR	transthyretin	NG_009490	None	None	None	None	None
LMNA	lamin A/C	NG_008692	None	None	None	None	None
DES	desmin	NG_008043	None	None	None	None	None
LDB3	LIM domain binding 3 (ZASP)	NG_008876	None	None	None	None	None
TAZ	tafazzin	NG_009634	None	None	None	None	None
PLN	phospholamban	NG_009082	None	None	None	None	None

TTR	transthyretin	NG_009490	None	None	None	None	None
LAMP2	lysosomal-associated membrane protein 2	NG_007995	None	None	None	None	None
SGCD	delta sarcoglycan	NG_008693	None	None	None	None	None
MTTL1	mitochondrially encoded tRNAleucine 1	NC_012920_TRNL1	None	None	None	None	None
MTTQ	mitochondrially encoded tRNA glutamine	NC_012920_TRNQ	None	None	None	None	None
MTTH	mitochondrially encoded tRNAhistidine	NC_012920_TRNH	None	None	None	None	None
MTTK	mitochondrially encoded tRNA lysine	NC_012920_TRNK	None	None	None	None	None
MTTS1	mitochondrially encoded tRNA serine 1	NC_012920_TRNS1	None	None	None	None	None
MTTS2	mitochondrially encoded tRNA serine 1	NC_012920_TRNS2	None	None	None	None	None
MTND1	mitochondrially encoded NADH dehydrogenase 1	NC_012920_ND1	None	None	None	None	None
MTND5	mitochondrially encoded NADH dehydrogenase 5	NC_012920_ND5	None	None	None	None	None
MTND6	mitochondrially encoded NADH dehydrogenase 6	NC_012920_ND6	None	None	None	None	None
KCNQ1	potassium voltage-gated channel, KQT-like subfamily, member 1	NC_000011.9	None	None	G269S	None	None
KCNH2	potassium voltage-gated channel, subfamily H (eag-related), member 2	NC_000007.13	None	None	None	None	None
SCN5A	sodium channel, voltage-gated, type V, alpha subunit	NC_000003.11	None	None	None	None	None
ANK2	ankyrin 2, neuronal	NC_000004.11	None	None	None	None	None
KCNE1	potassium voltage-gated channel, Isk-related family, member 1	NC_000021.8	None	None	None	None	None
KCNE2	potassium voltage-gated channel, Isk-related family, member 2	NC_000021.8	None	None	None	None	None
KCNJ2	potassium inwardly-rectifying channel, subfamily J, member 2	NC_000017.10	None	None	None	None	None
CACNA1C	calcium channel, voltage-dependent, L type, alpha 1C subunit	NC_000012.11	None	None	None	None	None
CAV3	caveolin 3	NC_000003.11	None	None	None	None	None
SCN4B	sodium channel, voltage-gated, type IV, beta subunit	NC_000011.9	None	None	None	None	None
AKAP9	A kinase (PRKA) anchor protein (yotiao) 9	NC_000007.13	None	None	None	None	None
SNTA1	syntrophin, alpha 1	NC_000020.10	None	None	None	None	None
KCNJ5	potassium inwardly-rectifying channel, subfamily J, member 5	NC_000011.9	None	None	None	None	None

Supplemental Table 3. Panel of cardiac ion channel-related transcripts used for quantitative RT- PCR

	Gene	ASSAY ID	Gene description
1	GADPH	Hs99999905_m1	Glyceraldehyde-3-phosphate dehydrogenase
2	SCN5A	Hs00165693_m1	Nav1.5
3	KCND3	Hs00542597_m1	Kv4.3 (I_{to})
4	CACNA1C	Hs00167681_m1	$Ca_v1.2$
5	KCNH2	Hs04234270_g1	Kv11.1 (hERG/I_{kr})
6	KCNQ1	Hs00923522_m1	Kv7.1, α-subunit of I_{ks}
7	KCNA5	Hs00266898_s1	Kv1.5
8	HCN2	Hs00606903_m1	Hyperpolarization-activated cyclic nucleotide-gated channel (I_f)
9	HCN4	Hs00175760_m1	Hyperpolarization-activated cyclic nucleotide-gated channel (I_f)
10	KCNJ2	Hs00265315_m1	Inward rectifier K^+channel Kir2.1
11	KCNJ3	Hs01002552_m1	Inward rectifier K^+ channel Kir3.1
12	KCNJ5	Hs00942581_m1	Inward rectifier K^+ channel Kir3.4
13	KCNJ11	02625248_s1	ATP-sensitive inward rectifier K^+ channelKir6.2
14	KCNE1	Hs00897540_s1	minK, β-subunit of I_{ks}
15	KChIP2	Hs01552688_g1	β-subunit of I_{to}

Supplemental Table 4. Summary of action potential parameters in hESC-CMs and hiPSC-CMs

	% of cells	Beating rate (bpm)	MDP (mV)	Overshoot (mV)	APA (mV)	APD_{50} (ms)	APD_{70} (ms)	APD_{90} (ms)	V_{max} (V / s)
hESC-CMs									
Nodal-like	5	97 ± 12	-38.7 ± 2.8	32.4 ± 0.7	71.2 ± 1.7	142.5 ± 12.3	190.3 ± 16.7	242.7 ± 24.6	3.3 ± 0.6
Atrial-like	27	68 ± 5	-53.3 ± 1.0	45.6 ± 1.2	97.3 ± 1.3	178.6 ± 10.0	231.0 ± 10.4	298.5 ± 33.8	33.5 ± 8.7
Ventricular-like	68	48 ± 5	-57.2 ± 1.3	46.2 ± 2.3	101.1 ± 1.3	310.0 ± 14.2	320.6 ± 20.3	340.8 ± 38.7	25.1 ± 9.1
Normal hiPSC-CMs									
Nodal-like	8	75 ± 8	-34.3 ± 3.5	30.6 ± 1.1	65.1 ± 0.9	104.4 ± 20.2	204.7 ± 12.5	288.1 ± 25.5	3.4 ± 0.8
Atrial-like	29	48 ± 7	-47.2 ± 1.3	44.3 ± 1.8	90.7 ± 2.9	172.2 ± 12.3	220.4 ± 22.8	293.6 ± 20.3	28.9 ± 7.3
Ventricular-like	63	54 ± 9	-52.6 ± 0.7	46.0 ± 1.0	97.2 ± 1.3	326.4 ± 26.9	340.5 ± 14.6	370.2 ± 32.4	27.7 ± 5.3
LQT hiPSC-CMs									
Nodal-like	7	101 ± 11	-42.1 ± 1.7	29.9 ± 2.1	73.7 ± 4.1	187.6 ± 12.8	231.5 ± 17.5	283.0 ± 24.7	3.1 ± 0.4
Atrial-like	33	80 ± 9	-54.1 ± 1.3	48.4 ± 1.5	102.7 ± 4.7	416.3 ± 30.7***	467.3 ± 30.5***	514.7 ± 28.5***	31.1 ± 6.6
Ventricular-like	60	58 ± 4	-59.3 ± 0.8	50.0 ± 1.1	109.3 ± 1.8	821.5 ± 47.2***	839.4 ± 50.2***	884.2 ± 48.2***	25.9 ± 5.0
HCM hiPSC-CMs									
Nodal-like	5	82 ± 7	-31.9 ± 2.1	31.0 ± 2.2	61.6 ± 4.0	173.1 ± 21.2	213.8 ± 15.4	265.9 ± 25.5	2.1 ± 0.6
Atrial-like	28	63 ± 5	-52.7 ± 1.7	44.6 ± 1.1	97.5 ± 0.9	170.5 ± 11.8	217.7 ± 31.6	346.3 ± 40.5	30.4 ± 8.6
Ventricular-like	67	50 ± 2	-54.9 ± 0.7	48.8 ± 0.7	103.0 ± 1.0	374.5 ± 16.7	408.2 ± 21.5	426.1 ± 17.6	27.9 ± 7.9
DCM hiPSC-CMs									
Nodal-like	5	68 ± 15	-31.8 ± 2.3	30.7 ± 1.5	62.5 ± 1.4	169.6 ± 16.5	192.4 ± 21.8	240.8 ± 31.6	2.3 ± 1.1
Atrial-like	27	64 ± 11	-48.7 ± 3.7	42.5 ± 2.7	91.4 ± 2.2	176.2 ± 14.0	222.6 ± 25.4	278.8 ± 26.3	23.3 ± 8.1
Ventricular-like	68	59 ± 9	-54.8 ± 1.6	49.4 ± 1.1	104.2 ± 1.7	381.1 ± 30.2	415.5 ± 31.4	435.8 ± 35.4	23.4 ± 7.9

Supplemental Table 5. Summary of drug-induced hERG tail current inhibition on HEK293 cells

	Dose (μM)	Inhibition of hERG Current (Δ%)	IC_{50} (μM)
Cisapride	0.001	8.0±4.0	0.032±0.003
	0.01	25.0±3.0	
	0.03	50.0±5.0	
	0.1	90.0±5.0	
	0.3	97.7±3.0	
	1	99.2±8.0	
Nicorandil	0.1	3.0±3.2	>100
	1	-5.4±4.2	
	10	6.2±6.3	
	100	10.7±5.4	
Verapamil	0.01	4.4±1.0	0.194±0.050
	0.1	37.7±3.0	
	0.3	55.0±5.0	
	1	89.4±2.0	
	10	96.2±0.4	
	100	98.8±0.3	
Alfuzosin	0.1	6.0±5.0	11.34±0.72
	1	10.0±5.0	
	3	16.0±7.0	
	10	47.0±10.0	
	30	92.0±0.6	

Supplemental Table 6. Summary of drug-induced effects on action potentials

	hESC-CMs (H9)		Control hiPSC-CMs		LQT hiPSC-CMs		HCM hiPSC-CMs		DCM hiPSC-CMs	
	Dose (μM)	APD_{90} (Δ%)	Dose (μM)	APD_{90} (Δ%)	Dose (μM)	APD_{90} (Δ%)	Dose (μM)	APD_{90} (Δ%)	Dose (μM)	APD_{90} (Δ%)
Cisapride	0.001	4.0±0.3	0.001	2.6±0.4	0.001	6.7±2.0	0.001	7.5±1.1*	0.001	5.0±0.6
	0.003	8.4 ± 1.2	0.003	7.9 ± 1.1	0.003	27.0±5.0**	0.003	36.0±5.8**	0.003	15.0±2.9
	0.01	32.0±5.0	0.01	30.5±5.4	0.01	50.0±5.0*	0.01	58.8±6.9**	0.01	40.0±3.4
	0.03	75.0±2.2	0.03	77.3±2.6	0.03	88.0±6.0/EAD*	0.03	100.0± 10.0/EAD**	0.03	70.0±4.6
	0.1	120.0±10.0	0.1	125.0±18.8	0.1	EAD	0.1	EAD	0.1	150.0±18.8
	0.3	EAD	0.3	EAD	0.3	EAD	0.3	EAD	0.3	EAD
Nicorandil	0.001	-5.7±2.9	0.001	-5.7±2.9	0.001	-	0.001	-	0.001	-
	0.01	-7.0±5.8	0.01	-7.0±5.8	0.01	-10.8±7.0	0.01	-8.2±8.1	0.01	-10.0±5.8
	0.1	-13.0±5.8	0.1	-10.0±5.8	0.1	-25.3±8.0**	0.1	-15.0±11.5	0.1	-20.3±5.8**
	0.3	-20.0±6.9	0.3	-17.0±6.9	0.3	-	0.3	-	0.3	-
	1	-23.8±7.5	1	-25.0±7.5	1	-36.2±12.0**	1	-28.0±5.8	1	-22.7±7.5
	10	-51.7±11.5	10	-48.4±11.5	10	-71.6±10.0**	10	-51.0±11.5	10	-61.0±11.5*
Verapamil	0.1	5.0±8.7	0.1	2.5±5.8			-	-	-	-
	1	7.0±7.5	1	5.0±8.7			-	-	-	-
	3	10.0±8.0	3	10.0±7.0			-	-	-	-
	10	26.0±6.4	10	25.3±5.8			-	-	-	-
	30	27.0±8.0	30	25.8±10.0			-	-	-	-
Alfuzosin	0.1	0.3 ± 1.2	0.1	-1.4±4.6			-	-	-	-
	0.3	3.2 ± 4.1	0.3	4.1±5.2			-	-	-	-
	1	14.2 ± 6.7	1	18.9±5.8			-	-	-	-
	3	22.9 ± 5.3	3	25.8±6.9			-	-	-	-
	10	26.8 ± 9.4	10	27.2±8.7			-	-	-	-

Quantitative data are presented as mean ± s.e.m.. Comparison between the groups was performed by one-way analysis of variance (ANOVA), followed by the Dunnett test (for comparison of all groups to control hiPSC-CMs). * indicates *P* value of <0.05, ** indicates *P* value of <0.01

Supplemental Table 7. Panel of drugs used for drug screening on hESC-CMs and patient-specific hiPSC-CMs

Tested drugs	Phase target	Ion channel target	Current target	IC_{50} of hERG current inhibition (μM)	IC_{50} of APD prolongation/shortening (μM)			
					Control hiPSC-CMs	LQT-CMs	HCM-CMs	DCM-CMs
Cisapride	2, 3	hERG blocker	I_{Kr}	0.032 ± 0.003	0.035 ± 0.004	0.015 ± 0.007	0.014 ± 0.005	0.033 ± 0.006
Nicorandil	3	K-ATP channel opener	I_{Ks}	>100	13.44 ± 2.1	3.44 ± 1.11	11.45 ± 2.3	8.32 ± 1.35
Verapamil	2, 3	L-type Ca^{2+} channel blocker, hERG blocker	I_{Ca} I_{Kr}	0.194 ± 0.05	5.18 ± 2.6	-	-	-
Alfuzosin	1	Sodium channel ($Na_v1.5$) opener	I_{Na}	11.34 ± 0.72	2.12 ± 0.93	-	-	-